ISSN 2354-9114 (online), ISSN 0024-9521 (print)
Indonesian Journal of Geography Vol 57, No.2 (2025): 236-252
DOI: 10.22146/ijg.99395 website: https://jurnal.ugm.ac.id/ijg

INDONESIAN JOURNAL OF GEOGRAPHY

RESEARCH ARTICLE

Study of the Impact of Rainfall Pattern Dynamics on Carbon Monoxide and Nitrogen Dioxide Using Cloud Computing (Case Study in the Special Region of Yogyakarta, Indonesia)

Sadewa Purba Sejati, Rivi Neritarani

Faculty of Science and Technology, Universitas Amikom Yogyakarta, Indonesia

Received: 2024-08-24
Revised: 2025-01-02
Accepted: 2025-02-16
Published: 2025-05-26

Keywords: rainfall, carbon monoxide, nitrogen dioxide, cloud computing

Correspondent email: sadewa@amikom.ac.id

Abstract *Carbon monoxide (CO) and nitrogen dioxide (NO_2) are the primary pollutants found in the air. Based on the results of the study of predecessor researchers, it is known that human activity factors cause spatial and temporal changes in primary pollutants in the air, while natural factors, such as rainfall changes during the transition of seasons, have not been studied further. This study was conducted to examine the impact of rainfall changes on spatial patterns of primary pollutants (CO and NO_2). The Special Region of Yogyakarta (DIY), Indonesia was chosen as a research area. The data used were remote sensing data, namely CHRIPS (Climate Hazards Group InfraRed Precipitation with Station data, NRTI (Near Real Time) / L3_CO data, and NRTI / L3_NO_2 data. The data were analyzed using cloud computing methods based on Google Earth Engine and statistical analysis. The results showed that the dynamics of rainfall patterns had an impact on changes in CO and NO_2 concentrations although it was not significant. Based on the study, it is known that an increase in rainfall of 1% causes a decrease in CO concentration of 1.935 x 10^{-5} mol/m^2 and a decrease in NO_2* concentration of 3.151 x 10^{-9} mol/m^2. *A study conducted in southern India also concluded that higher rainfall has the potential to reduce CO and NO_2 concentrations. The impact of rainfall pattern dynamics presented quantitatively in this study is a new finding, because there have not been many studies that explain the impact of rainfall pattern dynamics on CO and NO_2 quantitatively.*

1. Introduction

Everyone needs to breathe clean air. Clean air has a good impact on human health and age (Li et al., 2023). Air is a geosphere object with spatial and temporal dimensions, meaning air quality varies based on space and time. Air pollution generally occurs due to anthropogenic activities that produce pollutants, such as carbon monoxide (CO) and nitrogen dioxide (NO_2) (Kwiecień & Szopińska, 2020). Spatial and temporal dynamics studies of air pollutants have been conducted intensively during the COVID-19 pandemic. Based on the study, it is known that air pollutants decrease significantly when *lockdowns* or large-scale social restrictions are imposed.

Nitrogen dioxide (NO_2) pollutants decreased significantly during *the lockdown* in Turkey (Ghasempour et al., 2021). Carbon monoxide (CO) and nitrogen dioxide ($NO_{2)}$ also declined as lockdowns were implemented in some parts of India (Halder et al., 2023). A decrease in pollution has also occurred during the COVID-19 pandemic in 2020, especially in the Jakarta, Surabaya, and Yogyakarta areas (Khasanah & Nucifera, 2022; Rendana et al., 2022; Suhardono et al., 2023). Some predecessor researchers also stated that the number of pollutants in China tended to decline in China, Bangladesh, and Tehran during the COVID-19 pandemic (Islam et al., 2021; Moradi & Zeuss, 2023; Xing et al., 2022). The decrease in air pollutants was caused by reduced use of motor vehicles during the lockdown. The reduced use of motor vehicles has decreased exhaust emissions from burning fossil fuels, so air pollutants are also reduced (Irwansyah et al., 2024).

Research on the spatial and temporal dynamics of air pollutants was carried out during the COVID-19 pandemic in 2020. Predecessor researchers tended to correlate changes in spatial patterns of air pollutants with large-scale social distancing policies (*lockdowns*). Air pollutants used as parameters vary, ranging from carbon monoxide, nitrogen dioxide, and sulfur oxides to micro-sized solids dispersed in the atmosphere. (Fardani et al., 2021; Khasanah & Nucifera, 2022; Xing et al., 2022). Based on the results of previous research, it is known that the concentration of air pollutants has decreased because *lockdowns* have suppressed human activities in the use of fossil fuels contained in various modes of transportation (Islam et al., 2021; Rendana et al., 2022).

Natural variability, such as rainfall, has not been widely used in studying the spatial dynamics of air pollutants. Based on data analysis using 200 publication manuscripts for 2020-2023 sourced from Google Scholar (Figure 1), it is known that the keyword air quality index (keywords used in air pollutant research) is closer to the keywords lockdown, pandemic, and human activity, while keywords related to rainfall (precipitation) have a longer distance from air quality index. Air quality and air quality index have the same concept. Air quality is a measure that indicates the amount of gaseous

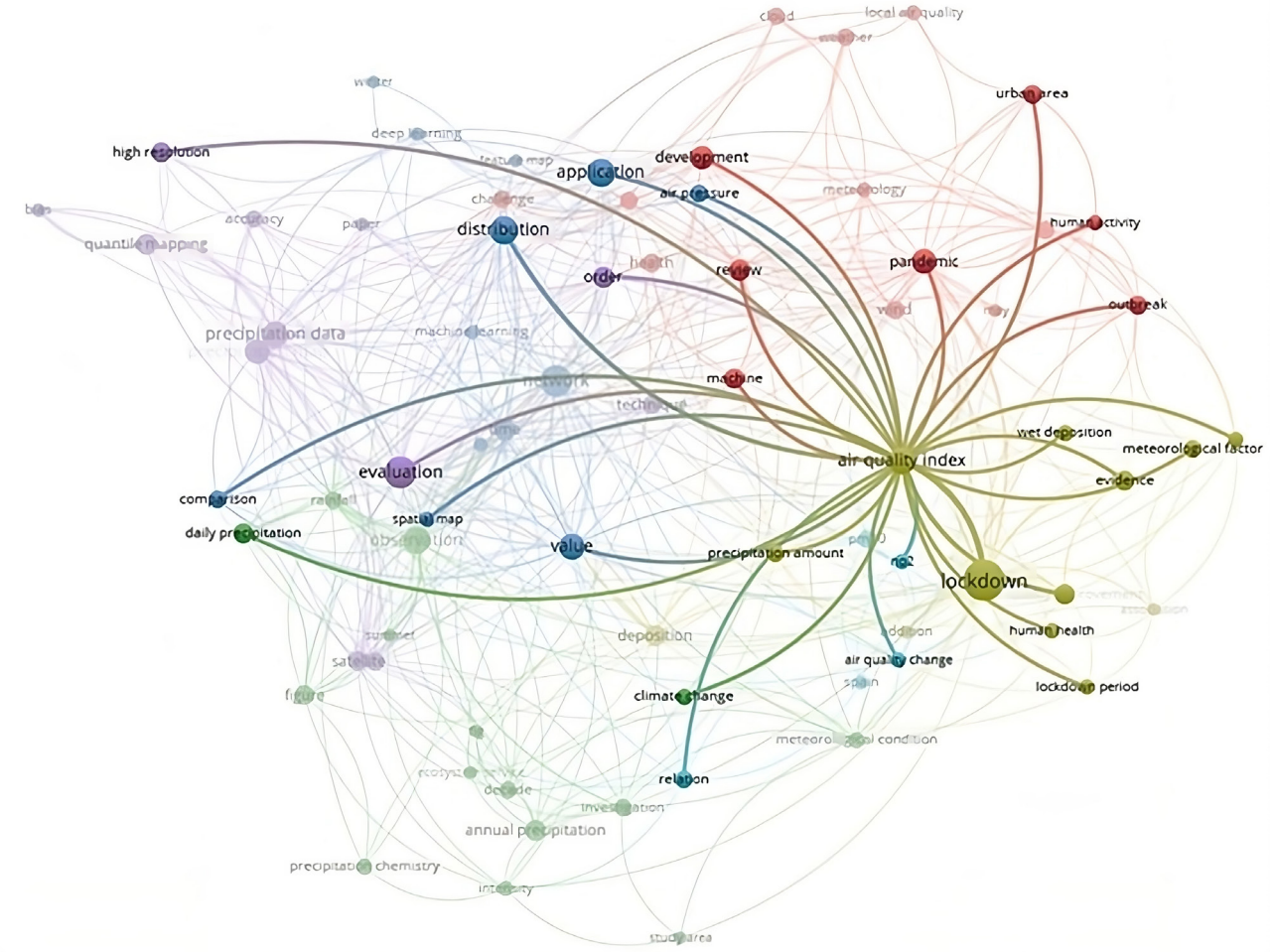

Figure 1. Results of Analysis of Recent Published Manuscripts (2020-2023) Related to Air Pollutants

pollutants and particulates in the air. The air quality index is a daily air quality report used to determine the impact of air quality on health (Cheremisinoff, 2002). Figure 1 also indicates that the use of rainfall variables in studying air pollutants has not been widely found.

Studies conducted by predecessor researchers focused on anthropogenic impacts on the spatial and temporal dynamics of air pollutants. Predecessor researchers tended to conclude that the decline in air pollutants was only due to reduced anthropogenic activity. Carbon monoxide (CO) and nitrogen dioxide (NO_2) are often used as objects of air pollution research in various regions locally and globally. Studies conducted in Latin American cities explain that the dynamics or fluctuations of NO_2 in the atmosphere are greatly influenced by anthropogenic factors, namely population mobility (Volke et al., 2023). Studies in some areas in Nigeria also show that fluctuations in CO and NO_2 are positively correlated with traffic density dynamics (Adedeji et al., 2016). A study conducted in Shandong Province, China also showed that the decline in mobility and community activities caused CO and NO_2 numbers to drop significantly (Xing et al., 2022). The decline in CO and NO_2 numbers also occurred in some areas of Ecuador due to the reduction in community mobility (Mejia et al., 2024).

Theoretically, rainfall as one of the components that shape weather and climate can dilute CO and NO_2 gases in the atmosphere. The statement that rainfall can dilute gas pollutants has often surfaced in various global studies. However, the question was not accompanied by an in-depth discussion about how much the dynamics of rainfall patterns affect the dynamics of CO and NO_2 gases. The impact of natural events, such as rainfall changes, on air pollutants has not been studied much, so references to the factors causing air pollutant dynamics are not comprehensive. This study was conducted to examine the impact of rainfall changes on spatial and temporal patterns of carbon monoxide (CO) and nitrogen dioxide (NO_2). The purpose of the study was achieved by analyzing the dynamics of daily rainfall, analyzing the dynamics of daily CO, analyzing the dynamics of daily NO_2, comparing the trends of rainfall, CO, and NO_2, by conducting statistical analysis.

The dynamics of rainfall, CO, and NO_2 were analyzed using daily data from October 2022 to March 2023. Spatial and temporal analysis was carried out using the cloud computing method with the google earth engine (GEE) program. GEE is a computer program based on java script. GEE can be used to extract rainfall, CO, and NO_2 data. GEE is also used to analyze data and visualize the results of data analysis spatially and temporally. Daily rainfall data is compared with daily CO data and daily NO_2 data to find out the trend. The impact of rainfall dynamics on CO and NO_2 is obtained by using linearity tests and scattergrams on statistical analysis.

2. Methods

The research was conducted in the Special Region of Yogyakarta (DIY) administrative area. DIY was chosen as the research location because the air quality was once below the quality standard (Cahyono, 2016; Dewi et al., 2020). The comparison of air quality measurement results in the field with

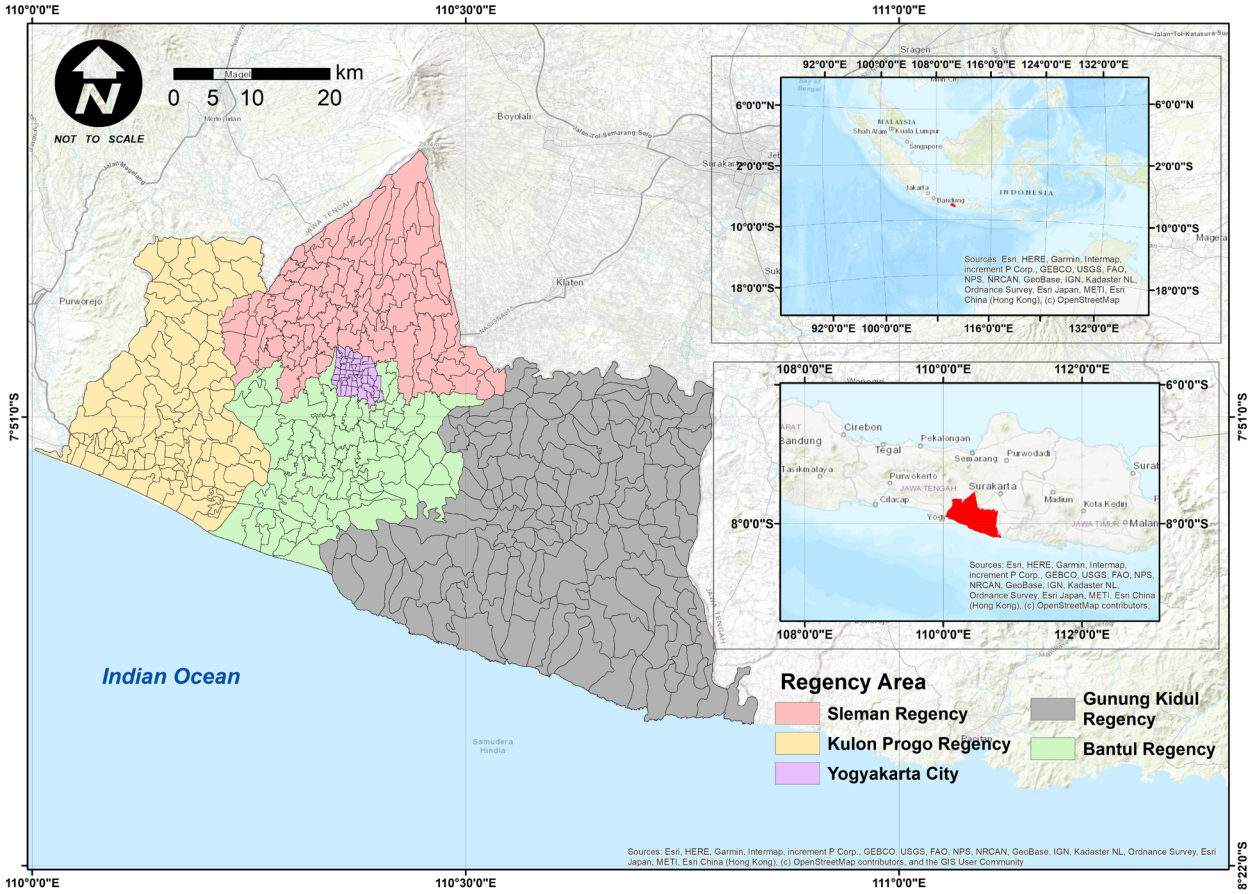

Figure 2. Research Area

air quality standards based on the Indonesian Government Regulation Number 41 of 1999 concerning national ambient air quality, show that SO_2 in some locations have exceed the quality standards, while NO_2 almost exceed the quality standards. The research area can be seen in Figure 2. The research area of the case study was chosen by the author because DIY has unique geographical conditions. DIY has a varied landform and is rarely found elsewhere. Previous researchers stated that the diversity of landforms in the research area resulted in the unique rainfall patterns formation. However the impact of the unique rainfall pattern in the research area has never been associated with the dynamics of nitrogen dioxide and carbon monoxide gas emissions.

The data used in this study included rainfall, carbon monoxide (CO), and nitrogen dioxide (NO_2). The temporal dimension of the data was from October 2022 to April 2023. The time period of October 2022 to April 2023 was chosen as the temporal dimension because, in that time frame, there was a change in rainfall patterns in the DIY region (BMKG, 2023).

Spatial and temporal patterns of rainfall, CO, and NO_2 were analyzed through *cloud computing* methods using *the Google Earth Engine* (GEE) platform. The cloud computing method was chosen due to its ability to access and analyze spatiotemporal CO, NO_2, and rainfall data contained in remote sensing satellite imagery (Bangsawan et al., 2021; Garajeh et al., 2023; Suharman et al., 2023). Most previous researchers also use cloud computing as an alternative provider of earth data. Cloud computing method is a considerable alternative to access institutional data, which are usually incomplete. JavaScript-based programming language is used to identify spatial and temporal patterns of rainfall, CO, and NO_2.

Rainfall data uses mm/day as measurement units while CO and NO_2 data use mol/m^2 units. Previouse researchers used mol/m^2 as measurement units to express the amount of CO and NO_2 using cloud computing based on Google Earth Engine (GEE), and did not convert the measurement unit of mol/m^2 to ppm (parts per million). Although the measurement unit of ppm is commonly used for gas concentrations, it is less suitable for satellite data, due to variations in altitude and variations in pressure and temperature (Halder et al., 2023; Rahaman et al., 2023; Suharman et al., 2023; Volke et al., 2023).

The data used to identify spatial patterns of rainfall is remote sensing satellite data CHIRPS (Climate Hazards Group Infra-Red Precipitation with Station) with a spatial resolution of 0.05^0 (Funk et al., 2015; Ocampo-Marulanda et al., 2022). The following is an excerpt of the script used to analyze rainfall in the research area.

```
var dataset     = ee.ImageCollection('UCSB-CHG/CHIRPS/
                  DAILY')
                  .select('precipitation').filterDate('2022-10-01',
                  '2023-04-30');
var DIY         = dataset.mean().clip(Yogyakarta)
var band_viz    = {min: 0,max: 15,palette: ['red', 'yellow',
                  'green', 'cyan' ,'blue']}; Map.addLayer(DIY,
                  band_viz, 'Mean Precipitation October 2022_
                  April_2023');
var title       = ui.Panel({style: {position: 'bottom-
                  center',padding:'8px 15px'}});
```

Spatial and temporal patterns of CO were identified using remote sensing data from NRTI/L3_CO (European et al. for Internal Market, 2013). The data were generated from the Sentinel 5P satellite conservation with a TROPOMI sensor (*tropospheric monitoring instrument*). The following is an excerpt of the script used to analyze CO data in the research area.

```
var dataset    = ee.ImageCollection('COPERNICUS/S5P/NRTI/L3_CO')
                 .select('CO_column_number_density').filterDate('2022-10-01', '2023-04-30');
var DIY        = dataset.mean().clip(Yogyakarta)
var band_viz   = {min: 0, max: 0.032,palette: ['black','blue','magenta','cyan', 'green', 'yellow', 'red']}; Map.addLayer(DIY, band_viz, 'October 2022_April_2023');
var title      = ui.Panel({style: {position: 'bottom-center',padding: '8px 15px'}});
```

Spatial and temporal patterns of NO_2 were identified using remote sensing data from NRTI/L3_NO_2 (European et al. for Internal Market 2013). The data were also generated from the Sentinel 5P satellite conservation with TROPOMI (*tropospheric monitoring instrument*) sensors. The following is an excerpt of the script used to analyze NO_2 data in the research area.

```
var dataset    = ee.ImageCollection('COPERNICUS/S5P/NRTI/L3_NO2')
                 .select('NO2_column_number_density').filterDate('2022-10-01', '2023-04-30')
var DIY        = dataset.mean().clip(Yogyakarta)
var band_viz   = {min: 0,max: 0.000065,palette: ['blue', 'purple', 'cyan', 'green', 'yellow', 'red']};Map.addLayer(DIY, band_viz, 'October 2022-April 2023');
var title      = ui.Panel({style: {position: 'bottom-center',padding: '8px 15px'}});
```

The results of the data analysis were visualized to see variations in rainfall, CO, and NO_2 in the research area. The visualizations are presented in the form of thematic maps and line graphs (diagrams). Thematic maps are used to present the spatial distribution of average CO, NO_2, and daily rainfall. The thematic map is compiled using data that has been extracted and analyzed using a java script-based cloud computing method. Data extraction and analysis were carried out with GEE, while the thematic map lay out process was carried out with the Arc GIS program version 10.8.

Graph visualization is used to present patterns of CO, NO_2, and rainfall fluctuations. The visualization in the form of a graph is prepared using CO, NO_2, and daily rainfall data that have been extracted and analyzed using the cloud computing method. In addition, graph visualization is also used to present daily fluctuation trends of CO, NO_2, and rainfall in the research area. The presentation of the graph visualization is done with the Microsoft Excel program.

The unit of analysis in this study is the satellite image pixels. The data used in this study are remote sensing images of Sentinel 5P NRTI CO, Sentinel 5P NRTI NO_2, and CHIRPS. Sentinel 5P NRTI CO and NO_2 remote sensing images have a spatial resolution of 5 km × 3.5 km (Ghasempour et al., 2021), while CHIRPS has a spatial resolution that is not much different, namely 5.3 km × 5.3 km (Ocampo-Marulanda et al., 2022). Based on the spatial resolution that have been described, the three satellite data have spatial resolutions that are not too different. So that the scale of data processing and analysis used in this study is simillar.

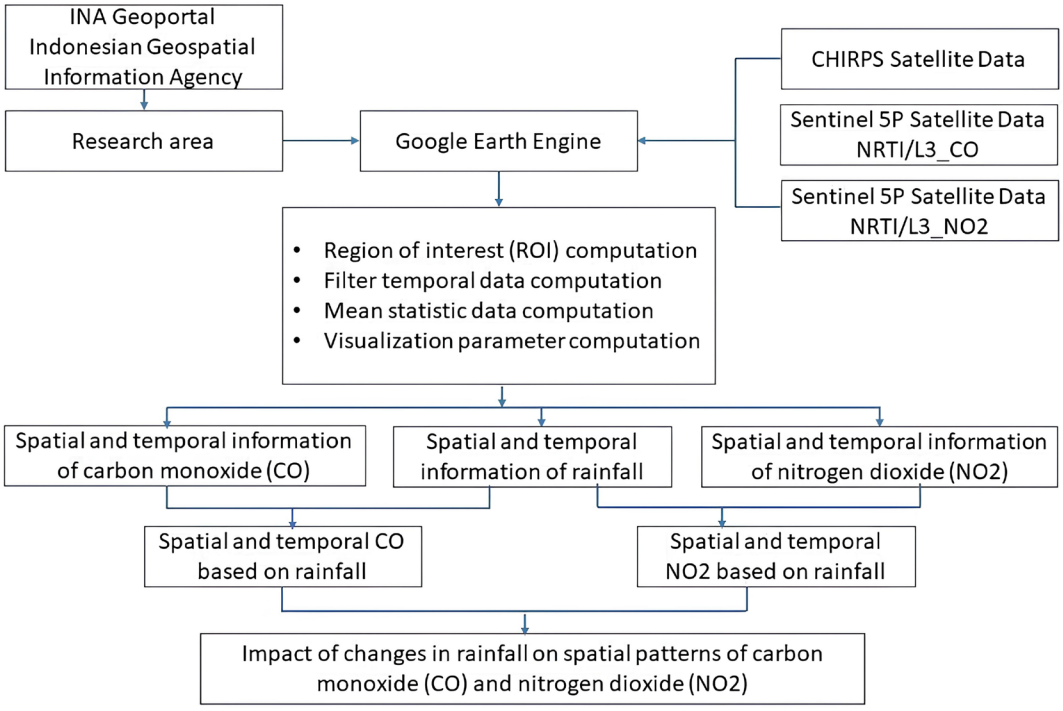

Figure 3. Research Flow Chart

The dynamic impact of rainfall patterns on CO and NO_2 was examined using statistical analysis, namely scattergram and linearity tests. The results of the data analysis were then explained descriptively using spatial and temporal approaches. The research flow chart can be seen in Figure 3.

3. Result and Discussion

Spatial Variation of Carbon Monoxide in Research Area

Based on the analysis of carbon monoxide data from October 2022 to April 2023, the highest mean amount of carbon monoxide was found around the Sentolo District, Kulon Progo Regency. The highest amount of carbon monoxide (CO) was 0.028 mol/m^2. The lowest amount, 0.019 mol/m^2, was found in the northern part of Sleman Regency, especially around the upper slopes of Merapi Volcano. The spatial pattern of CO in the research area can be seen in Figure 4. Based on previous studies, the concentration of CO in the atmosphere is caused by fossil fuel emissions from various activities, such as transportation, industry, and domestic activities (Liu et al., 2019; Suharman et al., 2023). Transportation activities have a significant impact on CO concentration in the atmosphere. Based on data presented by previous researchers (Figure 5 and Table 1), large-scale social restrictions that occurred in parts of South China resulted in a decrease in the transportation of people and goods. As a result, CO density also decreased. When social restrictions were relaxed, transportation activities slowly increased, then the CO concentration rate also increased. (Suharman et al., 2023).

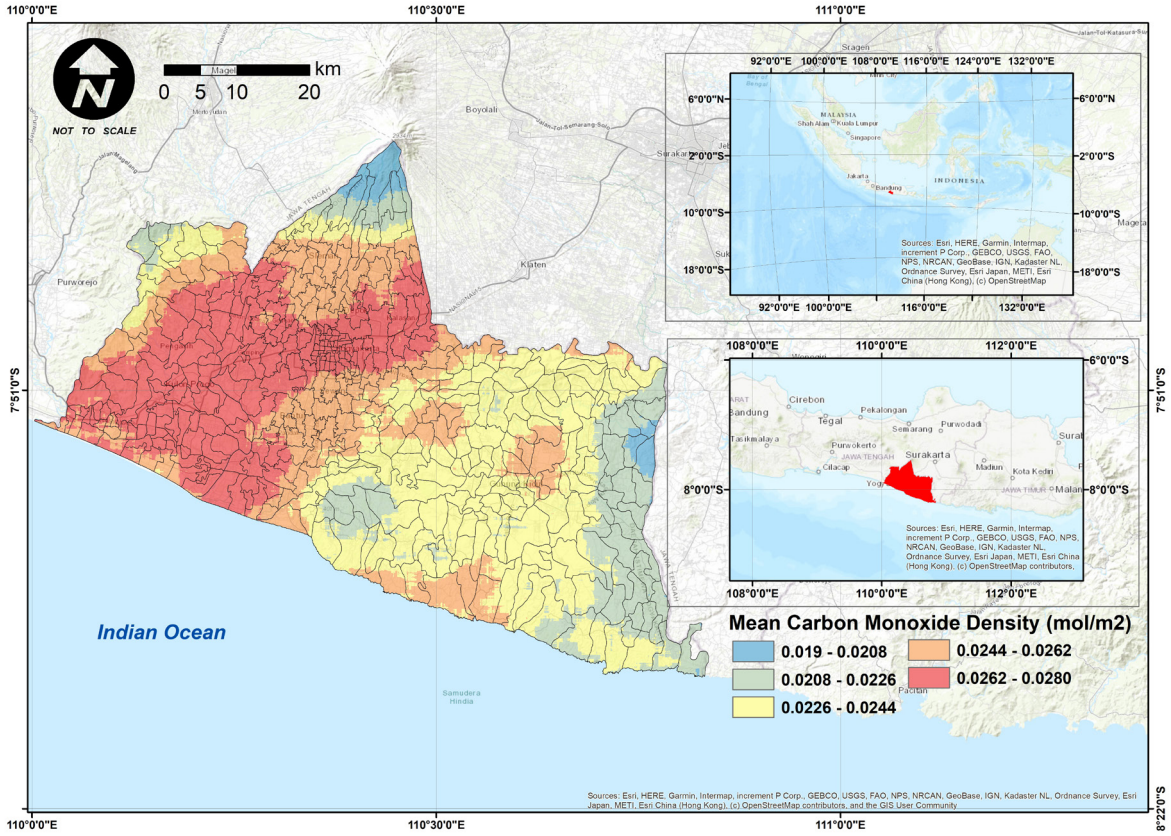

Figure 4. Spatial Patterns of Carbon Monoxide from October 2022 to April 2023 (Source: data processing, 2024)

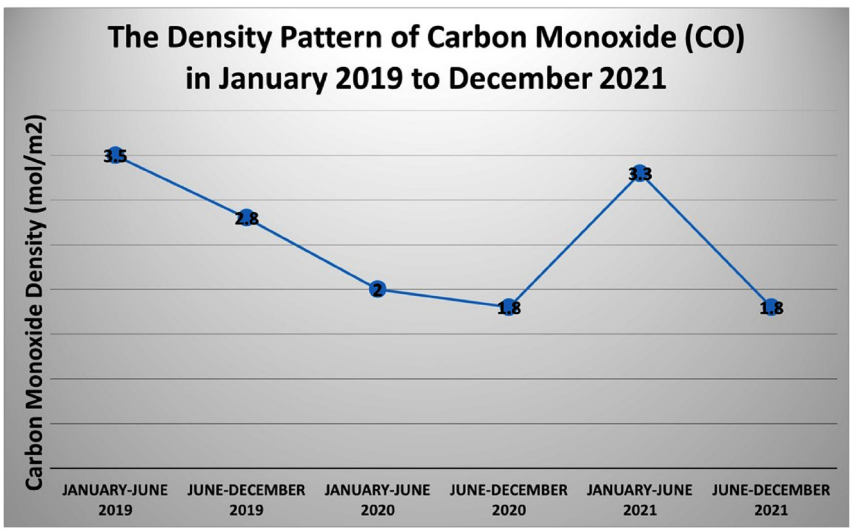

Figure 5. The Dynamics of Density Pattern of CO(Suharman et al., 2023)

Table 1. CO Dynamics Explanation Based on Figure 5

No	Time Period	CO Density (mol/m²)	Condition	Statement	Cause
1	January to June 2019	3.5	The highest density was located in coordinates 108.941 longitude and 10.547 latitude.	In this period, the research area was dominated by carbon monoxide with a density of 2 to 3.5 mol/m²	Massive Transportation
2	June to December 2019	2.8	The highest density was located in coordinates 110.490 longitude and 10.071 latitude.	The distribution of carbon monoxide patterns with a density of 2 to 3.5 mol/m² began to decrease, although it was not significant. In the period from June to December 2019, the research area was dominated by carbon monoxide in the range of 1 to 2.8 mol/m² density. Carbon monoxide density in the periode of June to December 2019 has indeed decreased, but in general the spatial pattern still tends to be simillar as the previous period.	Transportation begins to decline
3	January to June 2020	2	The highest density was located in coordinates 109.732 longitude and 8.564 latitude.	In the period of January to June 2020, no carbon monoxide cabron was found with a density exceeding 2 mol/m². Based on the results of data analysis, it is known that the density of carbon monoxide in this period is dominated by levels of 1 to 2 mol/m².	Restrictions on activities (lockdown) due to the covid-19 pandemic
4	June to December 2020	1.8	The highest density was located in coordinates 110.171 longitude and 10.342 latitude.	Activity restrictions due to the Covid-19 pandemic still have a significant effect on the spatial pattern of carbon monoxide density in the research area. In this period, the highest density is at 1.8 mol/m². The most dominant carbon monoxide density is in the range of 0.5 to 1.5 mol/m².	Restrictions on activities (lockdown) due to the covid-19 pandemic
5	January to June 2021	3.3	The highest density was located in coordinates 110.084 longitude and 10.73 latitude.	The density of carbon monoxide in the research area began to creep up. The highest density in the previous period (June to December 2020) was 1.8 mol/m², while in the period of January to June 2021 there was a significant increase which caused the highest density to be at 3.3 mol/m². Based on data visualization, it is known that the spatial pattern of carbon monoxide with a density of less than 2 mol/m² is decreasing, replaced by an increase in carbon monoxide with a density of more than 2 mol/m²	The relaxation of the lockdown that caused activities began to gradually normalize. Including activities in the research area.
6	June to December 2021	1.8	The highest density was located in coordinates 109.996 longitude and 9.886 latitude	Carbon monoxide density in June to December 2021 has decreased significantly compared to the previous period (January to June 2021). Based on data analysis, it is known that in the period of June to December 2021, the spatial pattern of carbon monoxide is dominated by carbon monoxide with a density of 0.5 to 1 mol/m²	This incident was caused by the re-enactment of large-scale restrictions due to the increase in Covid 19 cases globally.

Source: (Suharman et al., 2023)

Then, the authors compared the CO concentration in several districts in each regency in the research area. The comparison of CO concentrations was carried out in districts selected based on population density levels. Population density is used as a selection criterion, since the denser the population, the higher the level of service, industry and domestic activities related to the use of fossil fuels. The results of the comparison of CO levels in each district can be seen in Table 2. Based on Table 2, it is showed that the variation in CO concentration is very low. The results of the calculation showed that the CO concentration was below 0.1 mol/m², so a decimal fraction with a level of 1 x 10^{-3} is used to accommodate very low variations.

Based on Table 2, the CO concentration ranges from 0.026 to 0.034 mol/m². The top two districts with the highest CO concentrations are Sentolo (0.034 mol/m²) and Wates (0.028 mol/m²). Based on data from Indonesia Statistics (BPS) processed and published by the Department of Investment and One Stop Integrated Services or *Dinas Penanaman Modal dan Pelayanan Terpadu Satu Pintu* (2019), the highest population density, as seen in Table 2, is in Ngampilan District, with a

Table 2. CO Concentration in Several Districts in the Research Area

No	Regency/ City	Sub District	CO (mol/m^2)
1	Sleman Regency	Depok	0.027
2	Sleman Regency	Ngaglik	0.027
3	Sleman Regency	Gamping	0.027
4	Sleman Regency	Mlati	0.027
5	Sleman Regency	Kalasan	0.027
6	Gunung Kidul	Playen	0.026
7	Gunung Kidul	Karang Mojo	0.026
8	Gunung Kidul	Semin	0.026
9	Gunung Kidul	Ngawen	0.026
10	Gunung Kidul	Wonosari	0.027
11	Kulon Progo	Sentolo	0.034
12	Kulon Progo	Wates	0.028
13	Kulon Progo	Lendah	0.027
14	Kulon Progo	Galur	0.027
15	Kulon Progo	Nanggulan	0.027
16	Yogyakarta	Ngampilan	0.027
17	Yogyakarta	Gedong Tengen	0.027
18	Yogyakarta	Danurejan	0.027
19	Yogyakarta	Pakualaman	0.027
20	Yogyakarta	Wirobrajan	0.027
21	Bantul	Banguntapan	0.027
22	Bantul	Sewon	0.027
23	Bantul	Kasihan	0.027
24	Bantul	Bantul	0.027
25	Bantul	Pleret	0.026

Source : data processing, 2024

Tabel 3. Traffic Performance of Kulonprogo Region in 2022

No	District	Road Sections	Traffic Performance (V/C Ratio)			Average per year
			2020	2021	2022	
1	Wates	Nagung - Cicikan	0.77	0.52	0.61	0.63
2	Sentolo	Sentolo - Brosot	0.20	0.50	0.57	0.42
		Sentolo – Nanggulan	0.30	0.40	0.50	0.40
		Sentolo – Pengasih	0.20	0.19	0.21	0.20

Source : Transportation in Figures 2023 (Yogyakarta, 2023)

population density of up to 22,622 people/km^2. Sentolo and Wates Districts have lower population densities compared to Ngampilan District. The population density of Sentolo District is 910.27 people/km^2 (Sentolo, 2019) while Wates District is 1,238 people/km^2 (Wates, 2021).

Although the population density in Sentolo and Wates is lower than in Ngampilan, CO concentrations are in the two highest ranks. This is due to massive transportation activities in the two districts. According to Transportation in Figures 2023 of the Yogyakarta Transportation Agency, traffic performance in Wates District, especially on the Nagung – Cicikan road section, has experienced fluctuating changes from 2021 to 2022 (Table 3).

In 2020, the V/C ratio reached 0.77 and decreased in 2021 to 0.52. In 2022, the value of the V/C ratio increased to 0.61. These data show that the volume of vehicles on the road section is almost close to the available road capacity because the V/C Ratio value is almost close to 0.8 in accordance with the standard for calculating the exceeded road capacity. So it can be said that transportation activities in Wates District are quite massive. Meanwhile, in Sentolo District, transportation activities occur on three road sections, namely the Sentolo – Brosot, Sentolo – Nanggulan, and Sentolo – Pengasih road sectionss. According to Transportation in Figures 2023 of the Yogyakarta Transportation Agency, traffic performance on the Sentolo – Brosot road section experienced fluctuating changes from 2020 to 2022. In 2020, the V/C ratio reached 0.22 and increased in 2021 to 0.50. In 2022, the V/C ratio value also increased to 0.57. These data show that the volume of vehicles on the Sentolo – Brosot road section is almost close to the available road capacity because the V/C Ratio value is almost close to 0.8. Similar conditions also occur on the

Sentolo – Nanggulan road. Traffic performance on this road section has increased from 2020 to 2022. The V/C Ratio in 2020 was recorded at 0.30 and increased in 2021 to 0.40 and increased again in 2022 to 0.50. If calculated on average, the traffic performance in Sentolo District reaches 0.40 to 0.42 per year. This shows that indeed in Sentolo District there is quite massive transportation activity.

Massive transportation activity is the impact of the construction of Yogyakarta International Airport in Wates District, which is close to Sentolo District. Emissions from massive transportation activities have led to high CO concentrations (Adedeji et al., 2016; Setyono et al., 2020). The research results also showed that CO concentration levels were influenced by vegetation. Areas dominated by vegetation, such as the middle to upper slopes of Merapi Volcano and most of Gunung Kidul Regency, had relatively lower CO concentrations compared to areas with sparse vegetation. The slopes of Merapi Volcano have a CO concentration of 0.019 mol/km^2, while the CO concentration in Gunungkidul Regency is usually at 0.026 mol/km^2. This is because vegetation can reduce CO concentration (Benedict, 2023).

The CO pattern from October 2022 to April 2023 throughout the Special Region of Yogyakarta can be seen in Figure 6.

Based on the research results, the CO concentration varied from October 2022 to April 2023. Figure 6 shows that at the beginning of the research year, the CO concentration increased from November 5 to December 10, 2022.The CO concentration decreased after December 10, 2022, until the end of the year of research. The lowest CO concentration was on April 22, 2023. The graph also shows that despite variations, in general, the CO concentration throughout the years of the research experienced a downward trend.

Spatial Variation of Nitrogen Dioxide in Research Area

Second, based on data processing and analysis, the highest mean amount of nitrogen dioxide (NO_2) from October 2022 to April 2023 is 0.000082 mol/m^2 (Figure 7). The dominance of the highest amount of nitrogen dioxide was found in most parts of Sleman Regency. The highest concentration of NO_2 was found in Depok District, Sleman Regency. Meanwhile, the lowest concentration of NO_2 was found in Rongkop District, Gunung Kidul Regency, which is 0.00002 mol/m^2.

The author compared the average values of NO_2 concentration in several sub-districts in the research area (Table 4).

Based on data comparison, the highest NO_2 concentration was in the Sleman Regency, including Depok, Ngaglik, Mlati, Gamping, and Kalasan Districts. It is irrelevant if population density is considered the sole factor to explain the cause of high NO_2 concentrations. Based on population data published by the Bappeda (Regional Planning and Development Agency) of the Special Region of Yogyakarta (Yogyakarta, 2023), the population density in Sleman Regency from 2020 to 2023 was at 1,900 to 2,000 people/km^2, while in the same period, the population density of Yogyakarta City was at 11,500 people/km^2. If the NO_2 concentration is related to population density, the NO_2 concentration in Yogyakarta City should be higher than in Sleman Regency. Based on the comparison of NO_2 concentrations, it can be said that the existence of vegetation in the Sleman Regency area cannot absorb all NO_2, so the amount of NO_2 in the Sleman Regency is higher than in other areas. Compared with the CO distribution pattern (Figure 4), the NO_2 distribution pattern (Figure 7) is more centralized. This may be because the molecular weight of NO_2 is greater than CO's. The molecular weight of NO_2 is 46.006 g/mol (Medicine, 2024a), while the molecular weight of CO is 28.010 g/mol (Medicine, 2024b). The heavier molecular weight of NO_2 may cause NO_2 emissions to be less easily distributed widely by wind. Another factor that may influence the high NO_2 concentration in Sleman Regency and its surroundings is the volcanic activity of Merapi Volcano from late 2022 to early 2023. Previous research results stated that volcanic activity can be a source of NO_2 emissions in the atmosphere (Romanias

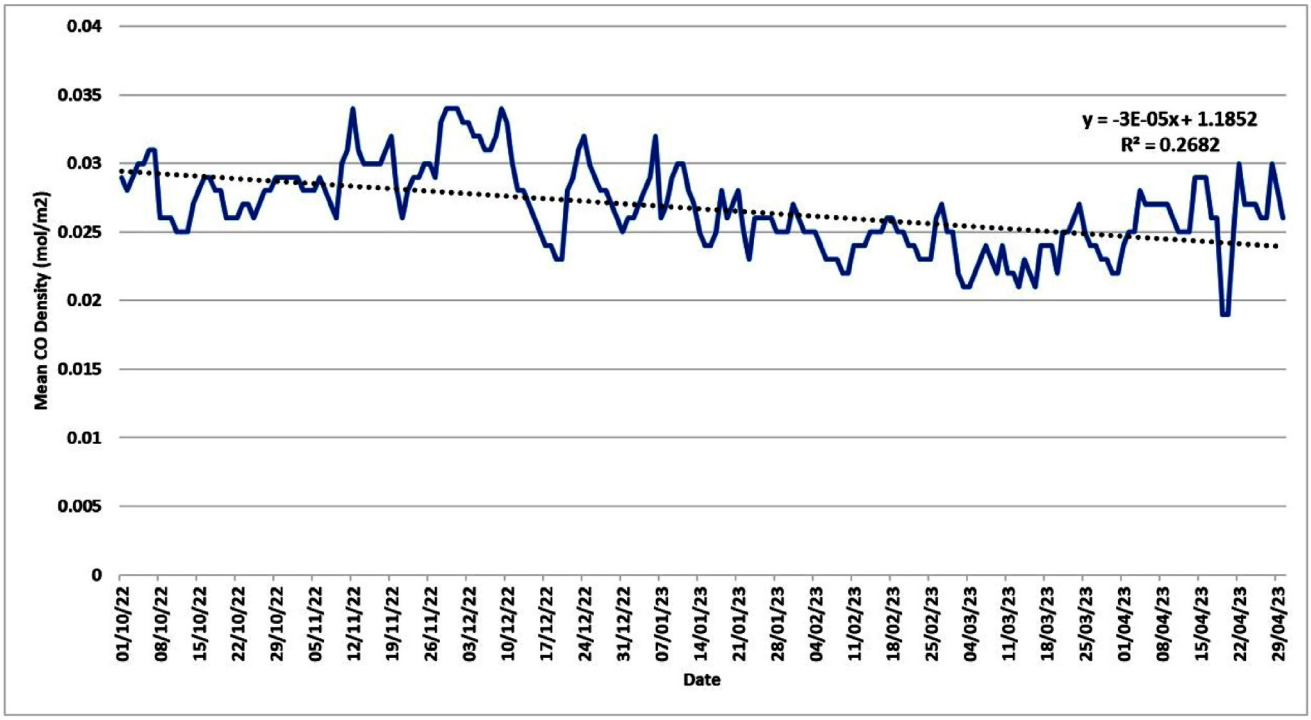

Figure 6. Carbon Monoxide Patterns from October 2022 to April 2023 (Source: data processing, 2024)

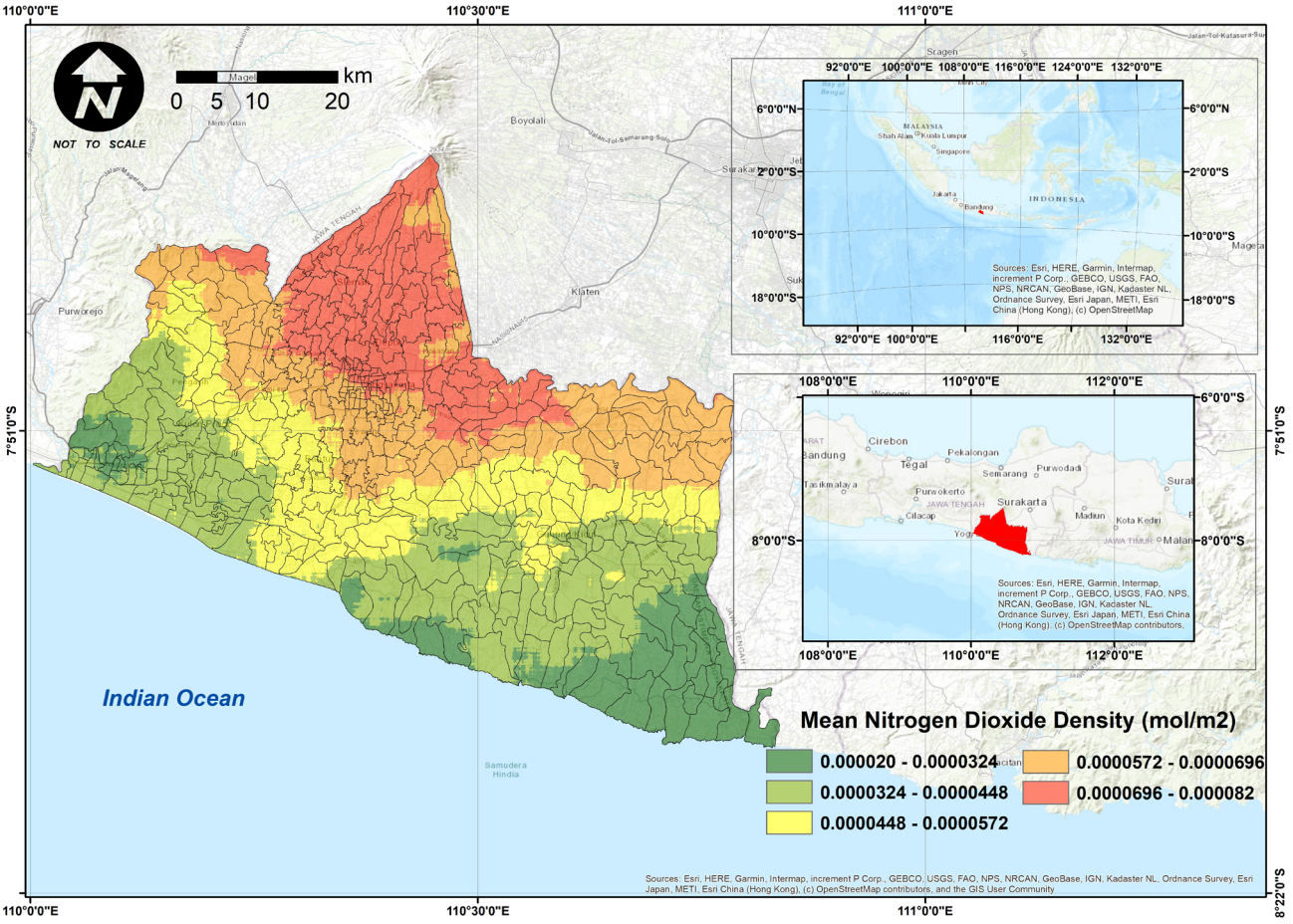

Figure 7. Spatial Patterns of Nitrogen Dioxide from October 2022 to April 2023 (Source: data processing, 2024)

et al., 2020). Based on the extraction of NO^2 data from the Sentinel 5P satellite, it is showed that from October 2022 to April 2023 the concentration of NO^2 around the Merapi Volcano fluctuated (Figure 8). NO^2 concentrations fluctuated from less than 0.00004 mol/m^2 to more than 0.00008 mol/m^2. The highest NO^2 concentrations occurred on November 15, 2022 at 0.000105 mol/m^2, November 20, 2022 at 0.000107 mol/m^2, January 17, 2023 at 0.000090 mol/m^2, January 29, 2023 at 0.000088 mol/m^2, and March 23, 2023 at 0.000088 mol/m^2.

The NO_2 pattern from October 2022 to April 2023 throughout the Special Region of Yogyakarta can be seen in Figure 9.

Based on the graph, NO_2 concentration in the year of the study varied. The highest daily average concentration was from 18 to 19 October 2022. After that, the NO_2 concentration decreased. NO_2 concentration increased again on November 25, 2022, December 24, 2022, and April 25, 2023. NO_2 concentration decreased drastically from January 30, 2023, to February 3, 2023. The graph shows that NO_2 is more variable than CO, but as with CO, in general, NO_2 concentration is trending downward.

Spatial Variation of Rainfall in Research Area

Based on the results of rainfall data analysis, the highest mean rainfall from October 2022 to April 2023 is 33.329 mm/day, spatially found in the northern part of Sleman Regency and the western part of Kulon Progo Regency. Several locations in Gunungkidul and Bantul Regencies, which are coastal areas, have the lowest mean rainfall of less than 10 mm/day. The visualization of rainfall patterns can be seen in Figure 9. The visualization of rainfall spatial pattern in Figure 9 is generated from the extraction and analysis of CHRIPS (Climate Hazards Center Infrared Precipitation with Station Data) data version 2.0. CHRIPS data extraction and analysis was carried out using cloud computing methods with a java script-based programming language.

Based on the results of data analysis, Pakem, Turi, Cangkringan, Samigaluh, Girimulyo, and Kokap Districts had higher rainfall than other districts. Pakem, Turi, and Cangkringan Districts are located in Sleman Regency, with a landform of the middle slope to the upper slope of the Merapi volcano. Samigaluh, Girimulyo, and Kokap Districts are located in Kulon Progo Regency with a landform dominated by denudational hill slopes. These districts are located at relatively higher elevations than other districts. This condition has the potential to cause orographic rain, which leads to higher rainfall intensity compared to other locations (Riasasi & Sejati, 2019; Sejati & Neritarani, 2024).

The rainfall pattern from October 2022 to April 2023 throughout the Special Region of Yogyakarta can be seen in Figure 10. During the year of the study, rainfall in the research area fluctuated. Based on data analysis, the highest average daily rainfall was from October 21, 2022, to November 18, 2022. From December 2022 to March 2023, rainfall fluctuated, with several peak rainfalls on December 23, 2022; January 24, 2024; and March 24, 2023. These rainfall peaks had lower rates compared to the peak rainfall rates in October and November 2022. The graph shows that rainfall experienced a decreasing trend from October 1, 2022, to April 30, 2023.

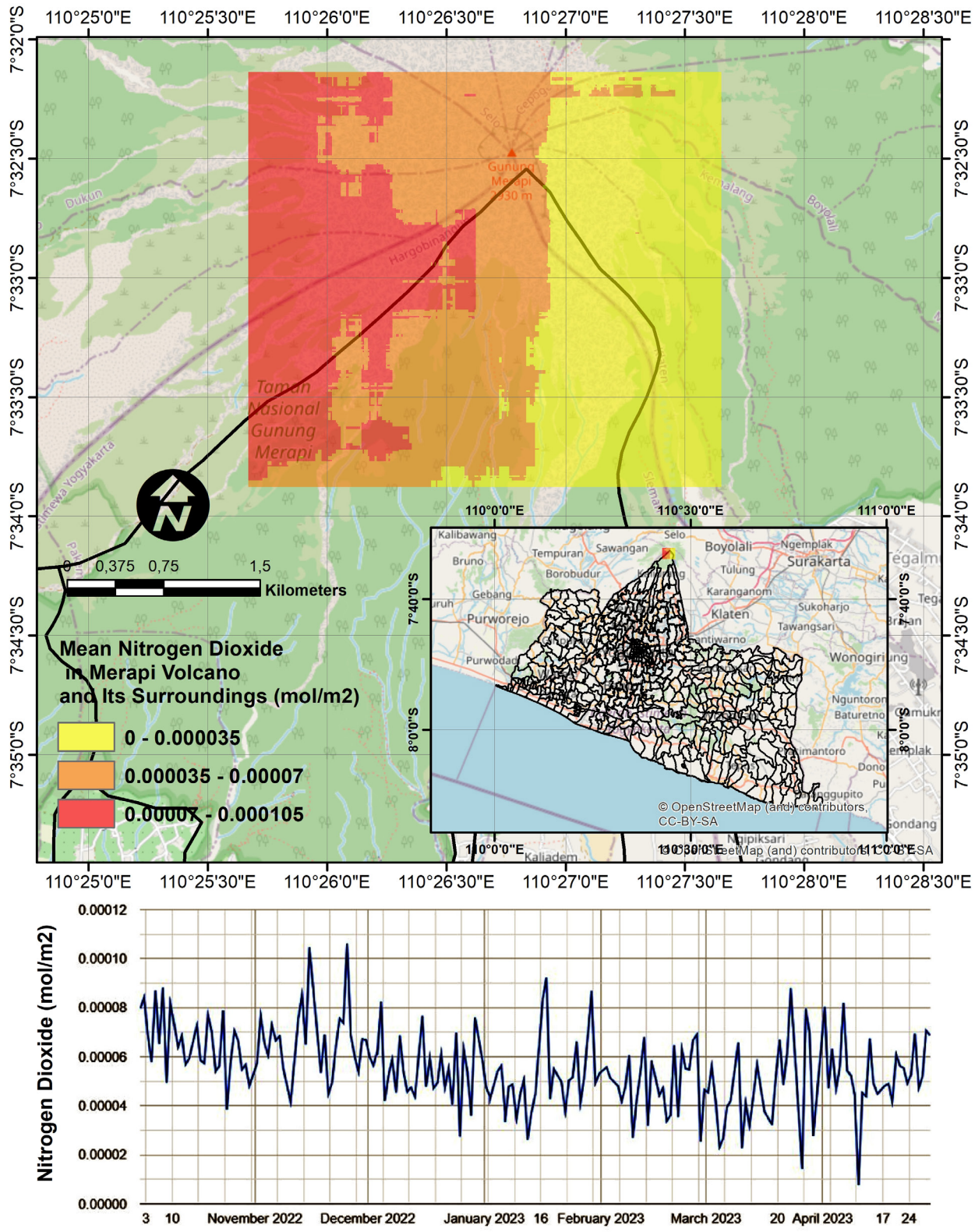

Figure 8. NO_2 data related to Merapi's volcanic activity from October 2022 to April 2023 (Source: data processing, 2024)

Impact of Rainfall Patterns on Carbon Monoxide and Nitrogen Dioxide

The impact of rainfall changes on the concentration of carbon monoxide (CO) and nitrogen dioxide (NO_2) in the air can be seen based on the correlation between the two variables. The correlation between these two variables was used to analyze the influence of one variable on another variable. Thus, correlation analysis per each affected variable was conducted to examine the impact of rainfall changes on carbon monoxide and nitrogen dioxide concentrations.

The impact of rainfall changes on carbon monoxide concentrations in the air was examined by assessing the data distribution patterns of the two variables in the form of scattergrams. Based on the scattergram analysis of the rainfall pattern fluctuation data variables and carbon monoxide (CO) concentration data variables in the research area from October 2022 to April 2023, the data patterns were irregular and tended to be random. This can be seen in the distribution of data patterns that do not lead to a linear line and tend to be scattered, which is shown in Figure 11.

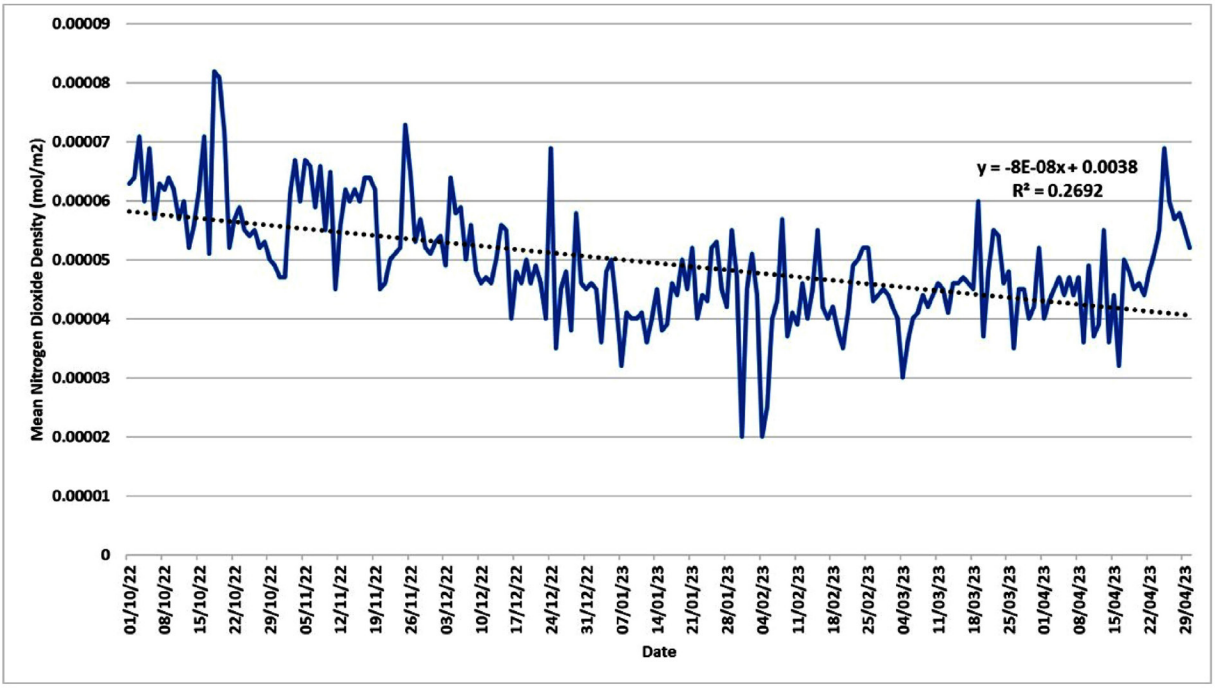

Figure 9. Nitrogen Dioxide Patterns from October 2022 to April 2023 (Source: data processing, 2024)

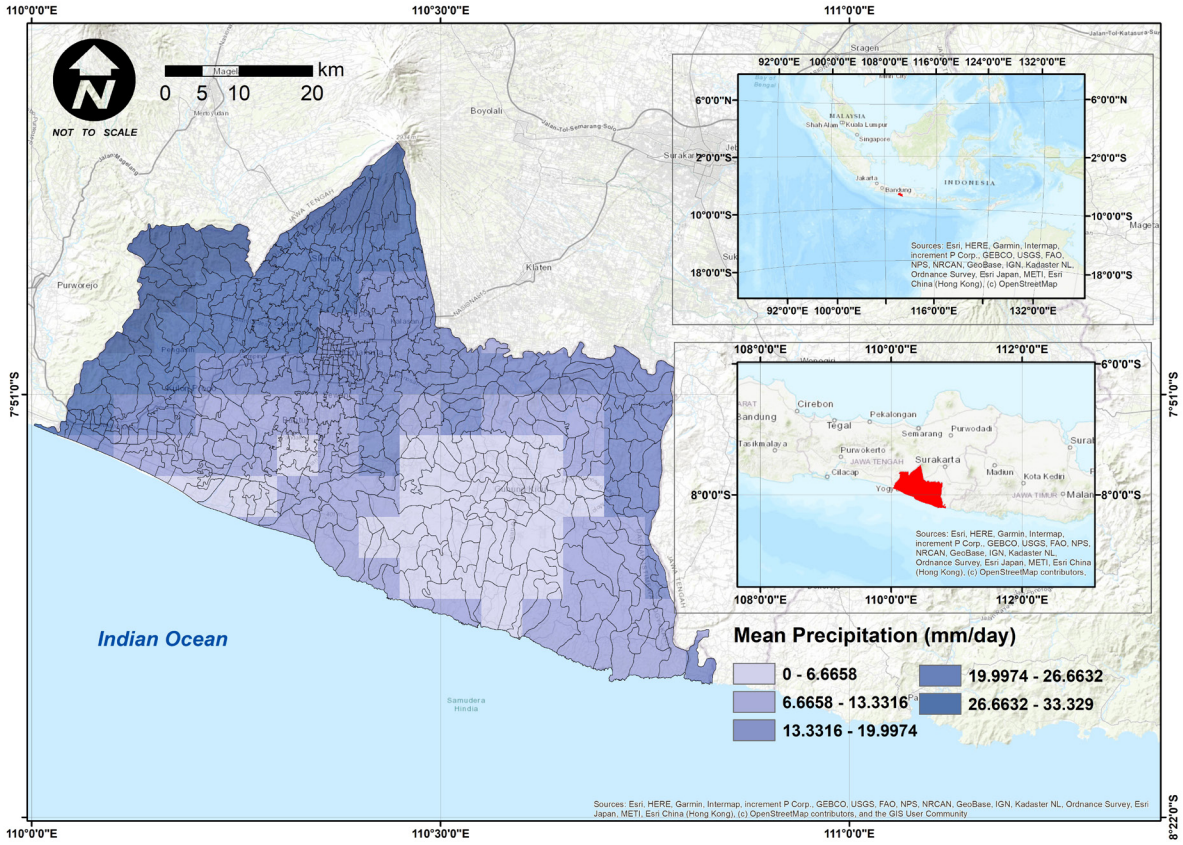

Figure 9. Spatial Patterns of Rainfall from October 2022 to April 2023 (Source: data processing, 2024)

Based on the scattergram, the data variables of rainfall pattern fluctuations and the data variables of carbon monoxide (CO) concentration in this research area may have a very weak correlation because they are not linear. However, the results of the linearity test carried out on these two variables showed different results. The significance value of deviation from linearity was 0.370, greater than the standard deviation of 0.05. Therefore, it can be concluded that there is a linear correlation between the rainfall fluctuation variable (independent) and the CO levels in the air (dependent). Based on the F test, the F count value was 1.379 while the F table for DF (198, 12) was 2.30. Since the F count is smaller than the F table, it can be concluded that there is a significant linear correlation between the rainfall fluctuation variables (independent) and carbon monoxide levels in the air (dependent). The results of this linearity test can be seen in Table 5.

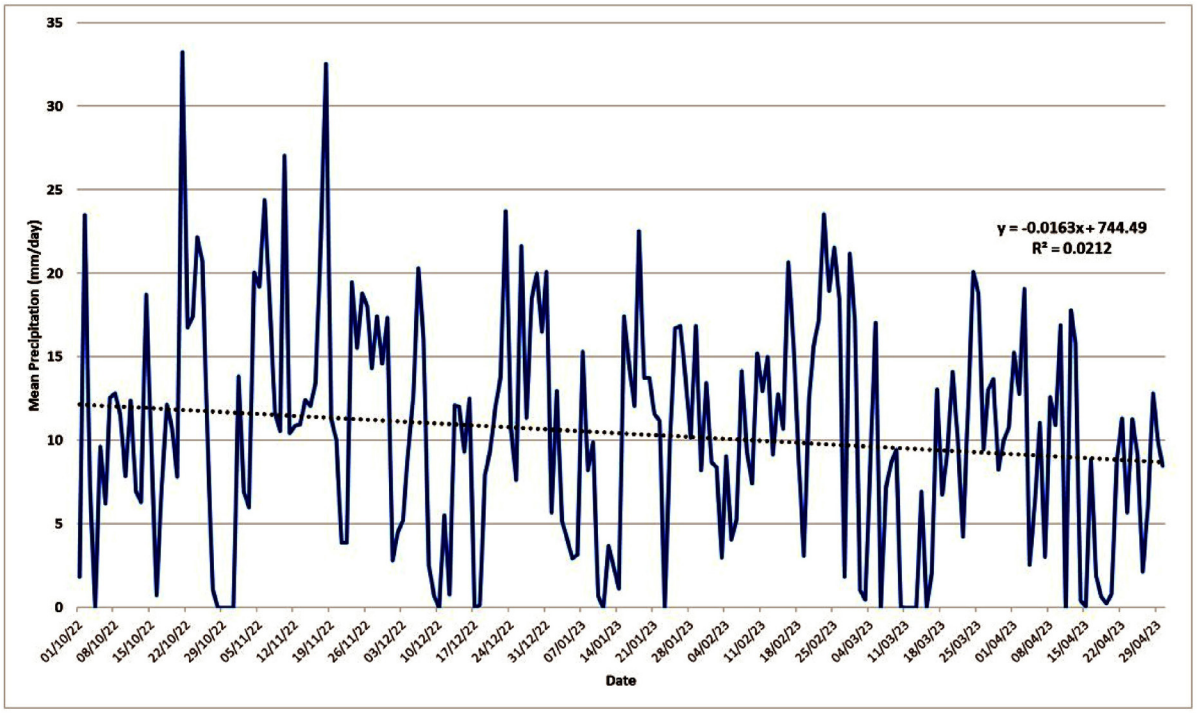

Figure 10. Rainfall Patterns from October 2022 to April 2023 (Source: data processing, 2024)

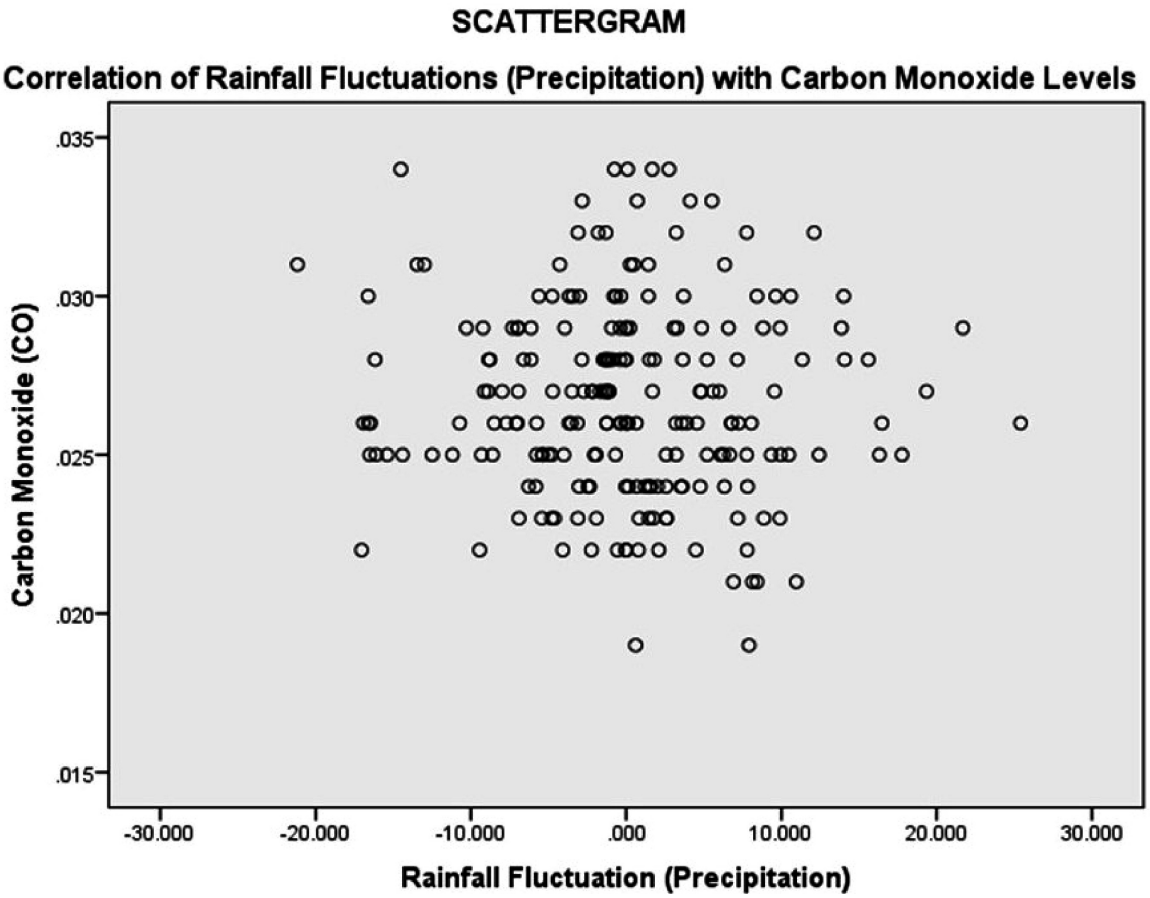

Figure 11. Scattergram Analysis of Rainfall Fluctuations (Precipitation) and Carbon Monoxide Levels Correlation

Based on the results of the linearity test, bivariate linear regression analysis can be carried out to examine the impact of increased rainfall on CO concentration in the air. Based on the results of the bivariate linear regression analysis, the regression equation obtained from the analysis is Y=0.027-0.00001935X. The coefficient a was 0.027, which means that if there is no rainfall change (rainfall fluctuation is zero), the consistent value of carbon monoxide levels in the air is 1.935 x 10^{-5} mol/m^2. Meanwhile, the coefficient b was -1.935 x 10^{-5}, which means that for every 1% increase in rainfall, the carbon monoxide levels will decrease by 1.935 x 10^{-5} mol/m^2. It shows that rainfall fluctuations negatively influence (cause a decrease)

the CO levels in the air. The results of the regression analysis can be seen in Table 6. Visualization of the comparison of rainfall patterns with CO patterns can be seen in Figure 12.

The impact of rainfall changes on the concentration of nitrogen dioxide in the air can be done by assessing the data distribution pattern of the two variables in the form of a scattergram. Based on the scattergram analysis of the rainfall pattern fluctuation data variables and the nitrogen dioxide (NO_2) concentration data variables in the research area from October 2022 to April 2023, the scattergram pattern of carbon monoxide concentration also showed irregular and random data. This can be seen in the distribution of data patterns that do not lead to a linear line and tend to spread out (scatter), which is shown in Figure 13.

Based on the scattergram, the rainfall pattern fluctuation data variable and the Nitrogen Dioxide (NO_2) concentration data variable in this research area may have a very weak correlation because they are not linear. However, the results of the linearity test conducted on these two variables showed different results. The significance value of deviation from linearity was 0.074, greater than the standard deviation of 0.05. Therefore, it can be concluded that there is a linear correlation between the rainfall fluctuation variable (independent) and the NO_2 levels in the air (dependent).

Table 5. Linearity Test Results between Rainfall Fluctuation and Carbon Monoxide Levels

			Sum of Square	df	Mean Square	F	Sig.
Carbon Monoxide (C0) * Rainfall Fluctuation (Precipitation)	Between Groups	(Combined)	.002	205	.000	1.375	.372
		Linearity	.000	1	.000	.681	.441
		Deviation from Linearity	.002	204	.000	1.379	.370
	Within Groups		.000	6	.000		
	Total		.002	211			

Table 6. Regression Analysis of Rainfall Fluctuation Impact to Carbon Monoxide (CO) Level

Model		Unstandardized Coefficients		Standardized Coefficients		
		B	Std. Error	Beta	t	Sig.
1	(Constant)	.027	.000		127.105	.000
	Rainfall Fluctuation (Precipitation)	-1.935E-5	.000	-.049	-.706	.481

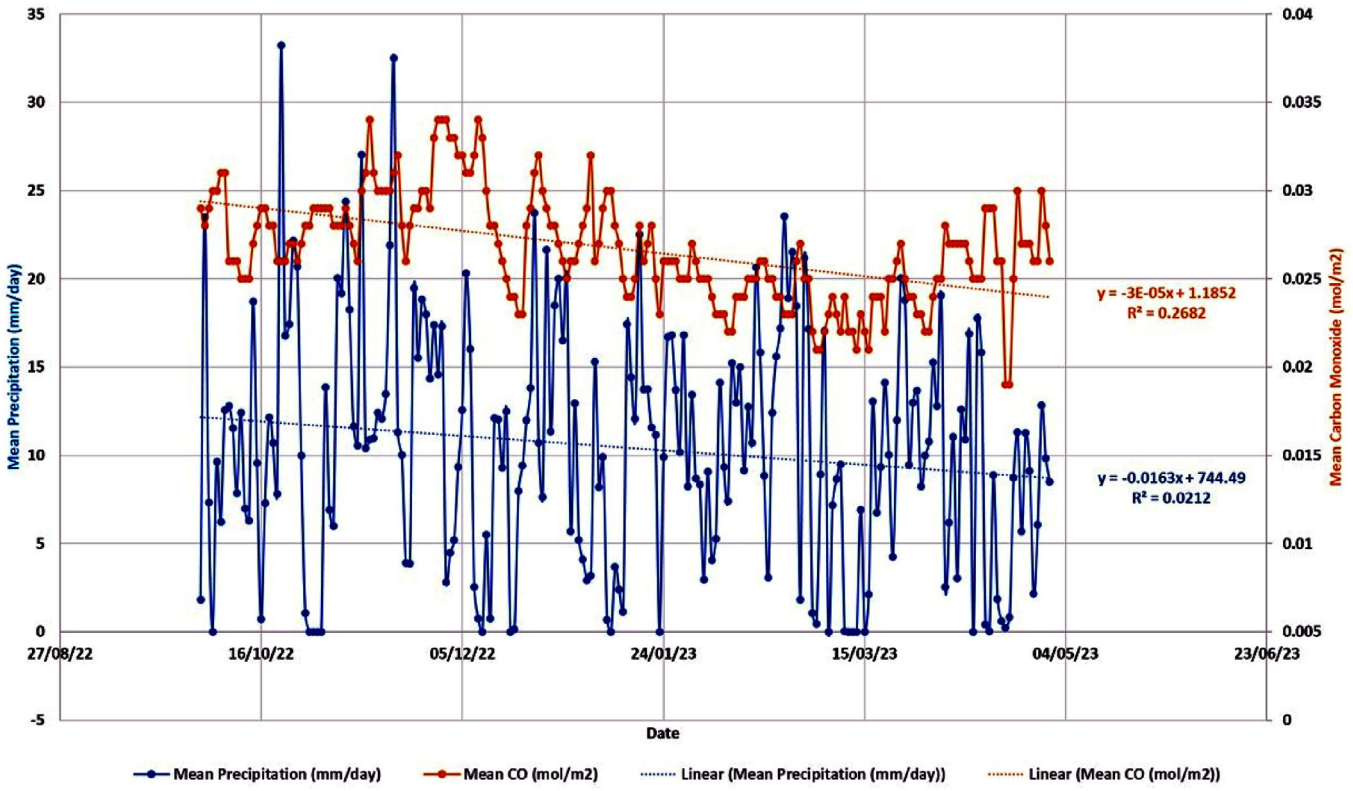

Figure 12. Visualization of Rainfall and Carbon Monoxide Patterns

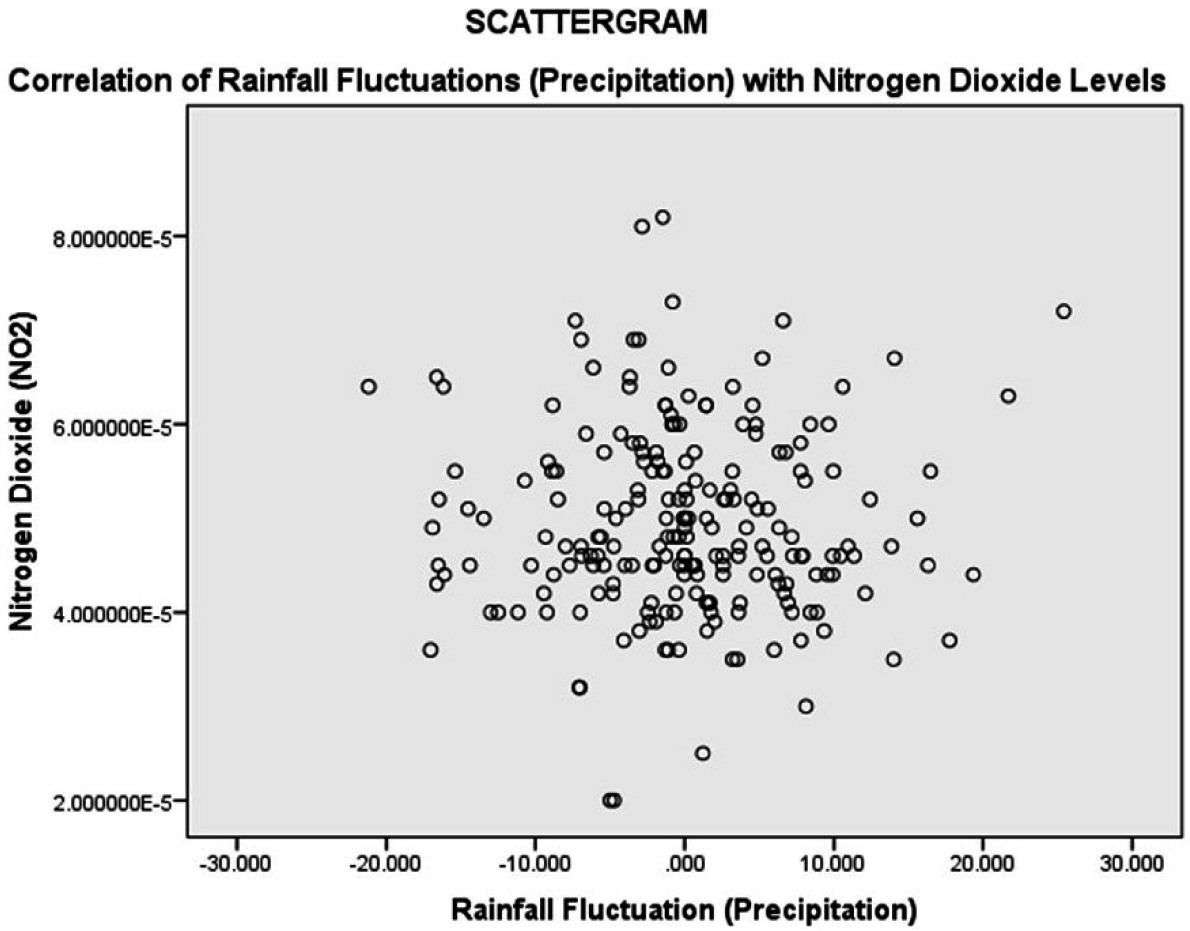

Figure 13. Scattergram Analysis of Rainfall Fluctuations (Precipitation) and Nitrogen Dioxide (NO_2) Levels Correlation

Table 7. Linearity Test Results between Rainfall Fluctuation and Nitrogen Dioxide Levels

			Sum of Square	df	Mean Square	F	Sig.
Nitrogen Dioxide (NO_2) * Rainfall Fluctuation (Precipitation)	Between Groups	(Combined)	.000	205	.000	3.116	.074
		Linearity	.000	1	.000	.004	.953
		Deviation from Linearity	.000	204	.000	3.131	.074
	Within Groups		.000	6	.000		
	Total		.000	211			

However, based on the F test, the F count was 3.131 while the F table for DF (198, 12) was 2.30. Since the F count is greater than the F table, it can be concluded that there is no significant linear correlation between rainfall fluctuation (independent variable) and nitrogen dioxide levels in the air (dependent variable). The results of this linearity test can be seen in Table 7.

Based on the results of the linearity test, bivariate linear regression analysis can be carried out to examine the impact of increased rainfall on the concentration of nitrogen dioxide in the air. Based on the results of the bivariate linear regression analysis, the regression equation is Y= $(4.942x10^{-5})$ – $(3.151x10^{-9})$ X. The coefficient a was 4.942 x 10^{-5}, meaning that if there is no rainfall change (rainfall fluctuation is zero), then the consistent value of nitrogen dioxide (NO_2) levels in the air is 4.942 x 10^{-5} mol/m^2. Meanwhile, the coefficient b was -3.151 x 10^{-9}, which means that for every 1% increase in rainfall, the nitrogen dioxide levels in the air will decrease by 3.151 x 10^{-9} mol/m^2. It shows that rainfall fluctuations negatively influence (cause a decrease) the levels of nitrogen dioxide in the air (NO_2) in the air. The results of the regression analysis can be seen in Table 8. Visualization of the comparison of rainfall patterns with NO_2 patterns can be seen in Figure 14.

Rainfall dynamics did not have a significant impact on the decrease in CO and NO_2 concentrations in the research area. The results showed that an increase in daily rainfall of 1% reduced the concentration of CO and NO_2 by 1,935 x 10^{-5} mol/m^2 and 3,151 x 10^{-9} mol/m^2. Geomorphologically, the research area can be said to be unique, because it has various land forms (Pohan et al., 2023). The diversity of landforms causes topographic conditions to vary. However, these variations did not have a significant impact on the difference in CO and NO_2 concentrations in the research area. For example, part of Kulon Progo Regency is denudational land with hilly topography that

Table 8. Regression Analysis of Rainfall Fluctuation Impact to Nitrogen Dioxide (NO2) Level

Model		Unstandardized Coefficients		Standardized Coefficients		
		B	Std. Error	Beta	t	Sig.
1	(Constant)	4.942E-5	.000		72.417	.000
	Rainfall Fluctuation (Precipitation)	-3.151E-9	.000	-.002	-.035	.972

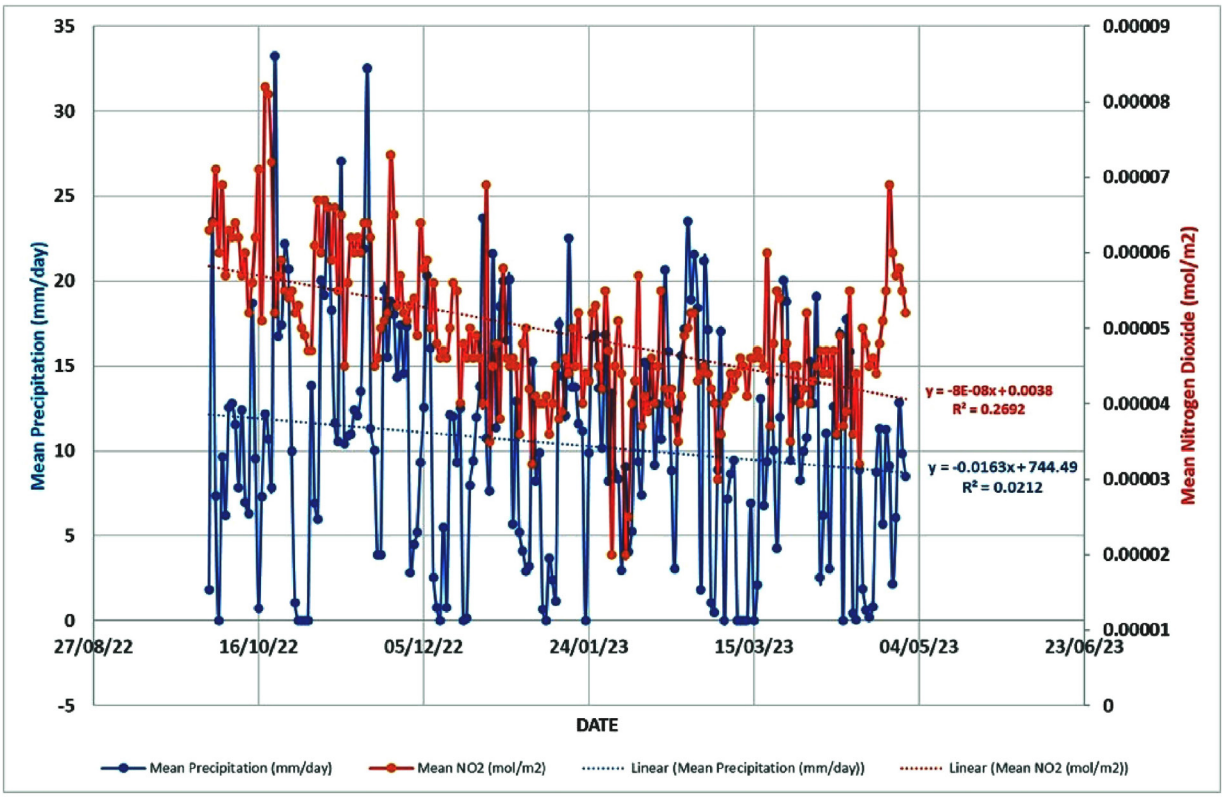

Figure 14. Visualization of Rainfall and Carbon Monoxide Patterns

has the potential to experience orographic rain (Rahmawati et al., 2021). Daily rainfall in Kulon Progo Regency reached 26.66 mm/day. Several areas of Sleman Regencies are also unique because they are formed by volcanic processes. The slopes in the area around the Merapi Volcano result in the potential for orographic rain (Rahmawati et al., 2021) with daily rainfall up to 33,329 mm/day. The geomorphological conditions of Kulon Progo Regency and Sleman Regency do result in relatively higher rainfall than other regions, such as Yogyakarta City, Bantul Regency, and Gunung Kidul Regency. However, the CO and NO_2 concentration in Kulon Progo Regency and Sleman Regency are not lower than Yogyakarta City, Bantul Regency and Gunung Kidul Regency.

The impact of rainfall dynamics on CO and NO_2 concentrations in the research area has not been comprehensively compared with various studies in other areas, because the simillar topic has not been widely studied. The study conducted in southern India is in line with the results achieved in this study, that although not significantly, the increase in rainfall has an impact on decreasing the concentration of CO and NO_2 gases in the atmosphere (Ayyamperumal et al., 2024). Studies conducted in Bangladesh, Polish cities, and Arak Cities in Iran also show that rainfall was not a dominant factor in the dynamics of CO and NO_2 concentrations (Garajeh et al., 2023; Haque et al., 2022; Kwiecien & Szopinska, 2020). Changes in CO and NO_2 concentrations are dominated by anthropogenic dynamics in the use of fossil fuels in various activities.

4. Conclusion

The results of the study show that cloud computing based on Google Earth Engine can be used to access, analyze, and visualize earth data related to gas emissions, such as carbon monoxide (CO) and nitrogen dioxide (NO_2). Cloud computing can also be used to access, analyze, and visualize rainfall data. Cloud computing can be used as a primary alternative in geospatial data mining, considering that accessibility and availability of institutional data are common obstacles in research.

The results of the study show that the concentrations of CO and NO_2 in the research area varied.

Partially, high CO concentration is found in research areas with massive transportation activities, such as near airports and routes to airports. High CO concentration is also found in locations with sparse vegetation cover. NO_2 concentration in the study also shows variations. High NO_2 concentration is found around the upper slopes to the middle slopes of Merapi Volcano. The high NO_2 concentration at the location may be influenced by the activity of Merapi Volcano. Based

on the research results, rainfall patterns also vary. The highest rainfall tends to occur on the middle to upper slopes of Merapi Volcano in Sleman Regency and the slopes of the denudational hills spatially distributed in Kulon Progo Regency. The rainfall rate on the upper slopes of Mount Merapi and the denudational hills in Kulon Progo Regency tends to be higher than other parts of the research area. This indicates that there is orographic rain on the upper slopes of the Merapi Volcano and the denudational hills in Kulonrpogo Regency.

Based on the research results, the dynamics of CO, NO_2, and rainfall experienced a downward trend from October 2022 to April 2023. The pattern of the decreasing trend of CO and NO_2 generally follows the dynamics of rainfall patterns. The results of the study show that every one percent increase in daily rainfall will reduce the concentration of CO by 1.935 x 10^{-5} mol/m^2 and reduce the concentration of NO_2 by 3.151 x 10^{-9} mol/m^2.

Acknowledgment

The authors would like to thank the Institute of Research and Community Service or *Lembaga Penelitian dan Pengabdian Masyarakat* (LPPM) of Universitas Amikom Yogyakarta for funding this research through contract number 8517/KONTRAK-LPPM/AMIKOM/XI/2023.

References

Adedeji, O. H., Oluwafunmilayo, O., & Oluwaseun, T. A. O. (2016). Mapping of traffic-related air pollution using GIS Techniques in Ijebu-Ode, Nigeria. *Indonesian Journal of Geography*, *48*(1), 76–86. https://doi.org/10.22146/ijg.12488

Ayyamperumal, R., Banerjee, A., Zhang, Z., Nazir, N., Li, F., Zhang, C., & Huang, X. (2024). Quantifying climate variation and associated regional air pollution in southern India using Google Earth Engine. *Science of The Total Environment*, *909*(2024), 168470. https://doi.org/https://doi.org/10.1016/j.scitotenv.2023.168470

Bangsawan, L., Satriagasa, M. C., & Bahri, S. (2021). Improved Performance of the CHIRPS Monthly Rainfall Estimation Extraction from Google Earth Engine (GEE) platform in South Sulawesi Region. In *IOP Conference Series: Earth and Environmental Science* (Vol. 893, pp. 1–9). IOP Publishing Ltd. https://doi.org/10.1088/1755-1315/893/1/012057

BAPPEDA Daerah Istimewa Yogyakarta. (2019). *Kependudukan Kota Yogyakarta (Population of Yogyakarta City)*. Retrieved from https://pmperizinan.jogjakota.go.id/web/kontent/71/kependudukan#:~:text=Penduduk yang paling padat berada,11.179 jiwa per Km2.

BMKG. (2023). Analsis Hujan Desember 2022 D.I. Yogyakarta. *Buletin Prakiraan Hujan Bulanan-Analisis Hujan Desember 2022-Prakiraan Hujan Februari, Maret, April 2023*, 42.

Cahyono, E. (2016). Penyebaran Pencemar Udara Di Kota Yogyakarta. In *Seminar Nasional Pendidikan dan Saintek* (Vol. 2016, pp. 2557–533). Retrieved from http://mirador.gsfc.nasa.gov/

Cheremisinoff, N. P. (2002). Introduction to Air Quality. *Handbook of Air Pollution Prevention and Control*. NASA'S Applied Remote Sensing Training Program. https://doi.org/10.1016/b978-075067499-7/50002-x

Dewi, A. L., Firmansyah, A., Hirma, E. S., Briliyanto, M. B. A., Fitri, M. N., & Nooraeni, R. (2020). Pengelompokkan Titik Wilayah di Provinsi Daerah Istimewa Yogyakarta Berdasarkan Kualitas Udara Menggunakan Algoritma Fuzzy C-Means. *Jurnal MSA (Matematika Dan Statistika Serta Aplikasinya)*, *8*(2), 1–12. https://doi.org/10.24252/msa.v8i2.16745

Fardani, I., Tarlani, & Aji, R. R. (2021). Analysis of Changes in Air Quality in Major Cities Indonesia during COVID 19 Using Remote Sensing Data. In *IOP Conference Series: Earth and Environmental Science* (Vol. 830, pp. 1–15). https://doi.org/10.1088/1755-1315/830/1/012085

Funk, C., Peterson, P., Landsfeld, M., Pedreros, D., Verdin, J., Shukla, S., … Michaelsen, J. (2015). The climate hazards infrared precipitation with stations - A new environmental record for monitoring extremes. *Scientific Data*, *2*(150066), 1–21. https://doi.org/10.1038/sdata.2015.66

Garajeh, M. K., Laneve, G., Rezaei, H., Sadeghnejad, M., Mohamadzadeh, N., & Salmani, B. (2023). Monitoring Trends of CO, NO2, SO2, and O3 Pollutants Using Time-Series Sentinel-5 Images Based on Google Earth Engine. *Pollutants*, *3*(2), 255–279. https://doi.org/10.3390/pollutants3020019

Ghasempour, F., Sekertekin, A., & Kutoglu, S. H. (2021). Google Earth Engine based spatio-temporal analysis of air pollutants before and during the first wave COVID-19 outbreak over Turkey via remote sensing. *Journal of Cleaner Production*, *319*(2021), 1–23. https://doi.org/10.1016/j.jclepro.2021.128599

Halder, B., Ahmadianfar, I., Heddam, S., Mussa, Z. H., Goliatt, L., Tan, M. L., … Yaseen, Z. M. (2023). Machine learning-based country-level annual air pollutants exploration using Sentinel-5P and Google Earth Engine. *Scientific Reports*, *13*(1), 1–19. https://doi.org/10.1038/s41598-023-34774-9

Haque, M. N., Sharif, M. S., Rudra, R. R., Mahi, M. M., Uddin, M. J., & Ellah, R. G. A. (2022). Analyzing the spatio-temporal directions of air pollutants for the initial wave of Covid-19 epidemic over Bangladesh: Application of satellite imageries and Google Earth Engine. *Remote Sensing Applications: Society and Environment*, *28*(10), 1–16. https://doi.org/10.1016/j.rsase.2022.100862

Irwansyah, M., Sunardi, E., Mulyo, A., & Sendjaja, Y. A. (2024). Air and noise pollution analyses near oil and gas fields in the Mahakam Delta, Kalimantan, Indonesia. *Indonesian Journal of Geography*, *56*(1), 148–157. https://doi.org/10.22146/ijg.87454

Islam, M. S., Tusher, T. R., Roy, S., & Rahman, M. (2021). Impacts of nationwide lockdown due to COVID-19 outbreak on air quality in Bangladesh: a spatiotemporal analysis. *Air Quality, Atmosphere and Health*, *14*(3), 351–363. https://doi.org/10.1007/s11869-020-00940-5

Khasanah, U. K., & Nucifera, F. (2022). The Effect of the COVID-19 Pandemic on Nitrogen Dioxide (NO2) Gas Concentration in Yogyakarta Special Province. In *2022 5th International Conference on Information and Communications Technology (ICOIACT)* (pp. 210–214). Yogyakarta. https://doi.org/10.1109/ICOIACT55506.2022.9971981

Kwiecien, J., & Szopinska, K. (2020). Mapping Carbon Monoxide Pollution of Residential Area in a Polish City. *Remote Sensing*, *12*(2885), 1–19.

Kwiecień, J., & Szopińska, K. (2020). Mapping carbon monoxide pollution of residential areas in a Polish City. *Remote Sensing*, *12*(18), 1–19. https://doi.org/10.3390/RS12182885

Li, X., Lyu, Y., Dong, W., & Xu, A. (2023). Exploring the relationship between air quality and health shocks to the elderly: A retrospective cross-sectional study in China. *Frontiers in Public Health*, *11*(1), 1–12. https://doi.org/10.3389/fpubh.2023.1087626

Liu, S., Fang, S., Liang, M., Sun, W., & Feng, Z. (2019). Temporal patterns and source regions of atmospheric carbon monoxide at two background stations in China. *Atmospheric Research*, *220*(January), 169–180. https://doi.org/10.1016/j.atmosres.2019.01.017

Mejía C, D., Faican, G., Zalakeviciute, R., Matovelle, C., Bonilla, S., & Sobrino, J. A. (2024). Spatio-temporal evaluation of air pollution using ground-based and satellite data during COVID-19 in Ecuador. *Heliyon*, *10*(7), 1–15. https://doi.org/10.1016/j.heliyon.2024.e28152

Moradi, A., & Zeuss, D. (2023). Investigation of the spatiotemporal patterns of air quality over the metropolitan area of Tehran, using TROPOMI and OMI data. *Air Quality, Atmosphere and*

Health, *17*(2024), 1–17. https://doi.org/10.1007/s11869-023-01450-w

Ocampo-Marulanda, C., Fernández-Álvarez, C., Cerón, W. L., Canchala, T., Carvajal-Escobar, Y., & Alfonso-Morales, W. (2022). A spatiotemporal assessment of the high-resolution CHIRPS rainfall dataset in southwestern Colombia using combined principal component analysis. *Ain Shams Engineering Journal*, *13*(5), 1–13. https://doi.org/10.1016/j.asej.2022.101739

Pohan, A. F., Sismanto, S., Nurcahya, B. E., Lewerissa, R., Koesuma, S., Saputro, S. P., … Adhi, M. A. (2023). Utilization and modeling of satellite gravity data for geohazard assessment in the Yogyakarta area of Java Island, Indonesia. *Kuwait Journal of Science*, *50*(4), 499–511. https://doi.org/10.1016/j.kjs.2023.05.016

Rahaman, S. N., Ahmed, S. M. M., Zeyad, M., & Zim, A. H. (2023). Effect of vegetation and land surface temperature on NO2 concentration: A Google Earth Engine-based remote sensing approach. *Urban Climate*, *47*(2), 1–16. https://doi.org/10.1016/j.uclim.2022.101336

Rahmawati, N., Rahayu, K., & Yuliasari, S. T. (2021). Performance of daily satellite-based rainfall in groundwater basin of Merapi Aquifer System, Yogyakarta. *Theoritical and Applied Climatology*, *146*(2021), 173–190.

Rendana, M., Idris, W. M. R., & Rahim, S. A. (2022). Changes in air quality during and after large-scale social restriction periods in Jakarta city, Indonesia. *Acta Geophysica*, *70*(5), 2161–2169. https://doi.org/10.1007/s11600-022-00873-w

Riasasi, W., & Sejati, S. P. (2019). Potential of Groundwater to Supply Domestic Water Necessity in Evacuation Shelters of Merapi Volcano Eruption. In *IOP Conference Series: Earth and Environmental Science* (pp. 1–11). IOP Publishing Ltd. https://doi.org/10.1088/1755-1315/271/1/012014

Sejati, S. P., & Neritarani, R. (2024). The Impact of Land Use Change on Groundwater Depth in The Groundwater Transition Zone of Merapi Volcano, Yogyakarta, Indonesia. *Indonesian Journal of Geography*, *56*(1), 96–115. https://doi.org/10.22146/ijg.88452

Sentolo, K. (2019). *Monografi Kapanewon Sentolo (Kapanewon Sentolo Monograph)*. Retrieved 04/19/2024 from https://sentolo.kulonprogokab.go.id/detil/157/monografi

Suhardono, S., Septiariva, I. Y., Rachmawati, S., Matin, H. H. A., Qona'ah, N., Nirwana, B., … Prayogo, W. (2023). Changes in the Distribution of Air Pollutants (Carbon Monoxide) during the Control of the COVID-19 Pandemic in Jakarta, Surabaya, and Yogyakarta, Indonesia. *Journal of Ecological Engineering*, *24*(4), 151–162. https://doi.org/10.12911/22998993/159508

Suharman, Y., Sejati, S. P., & Amirullah, I. (2023). Understanding the carbon monoxide threat in the South China Sea. *Regions and Cohesion*, *13*(3), 29–47. https://doi.org/10.3167/RECO.2023.130303

Volke, M. I., Abarca-del-Rio, R., & Ulloa-Tesser, C. (2023). Impact of mobility restrictions on NO2 concentrations in key Latin American cities during the first wave of the COVID-19 pandemic. *Urban Climate*, *48*(2), 1–16. https://doi.org/10.1016/j.uclim.2023.101412

Wates, K. (2021). *Monografi Kapanewon Wates (Kapanewon Wates Monograph)*. Retrieved from https://wates.kulonprogokab.go.id/detil/464/profil-2021

Xing, H., Zhu, L., Chen, B., Niu, J., Li, X., Feng, Y., & Fang, W. (2022). Spatial and temporal changes analysis of air quality before and after the COVID-19 in Shandong Province, China. *Earth Science Informatics*, *15*(2), 863–876. https://doi.org/10.1007/s12145-021-00739-7

Yogyakarta, D. P. P. (2023). *Transportasi Dalam Angka 2023. Laporan Transportasi dalam Angka 2023*.